



## Activation of anthrachamycin biosynthesis in *Streptomyces chattanoogensis* L10 by site-directed mutagenesis of *rpoB*<sup>\*#</sup>

Zi-yue LI<sup>1,2</sup>, Qing-ting BU<sup>1,2</sup>, Jue WANG<sup>1,2</sup>, Yu LIU<sup>3</sup>, Xin-ai CHEN<sup>1,2</sup>, Xu-ming MAO<sup>1,2</sup>, Yong-Quan LI<sup>†‡1,2</sup>

<sup>1</sup>Institute of Pharmaceutical Biotechnology & First Affiliated Hospital, School of Medicine, Zhejiang University, Hangzhou 310058, China

<sup>2</sup>Zhejiang Provincial Key Laboratory for Microbial Biochemistry and Metabolic Engineering, Hangzhou 310058, China

<sup>3</sup>College of Life Sciences, Zhejiang University, Hangzhou 310058, China

<sup>†</sup>E-mail: lyq@zju.edu.cn

Received June 26, 2019; Revision accepted Sept. 18, 2019; Crosschecked Nov. 1, 2019

**Abstract:** Genome sequencing projects revealed massive cryptic gene clusters encoding the undiscovered secondary metabolites in *Streptomyces*. To investigate the metabolic products of silent gene clusters in *Streptomyces chattanoogensis* L10 (CGMCC 2644), we used site-directed mutagenesis to generate ten mutants with point mutations in the highly conserved region of *rpsL* (encoding the ribosomal protein S12) or *rpoB* (encoding the RNA polymerase  $\beta$ -subunit). Among them, L10/RpoB (H437Y) accumulated a dark pigment on a yeast extract-malt extract-glucose (YMG) plate. This was absent in the wild type. After further investigation, a novel angucycline antibiotic named anthrachamycin was isolated and determined using nuclear magnetic resonance (NMR) spectroscopic techniques. Quantitative real-time polymerase chain reaction (qRT-PCR) analysis and electrophoretic mobility shift assay (EMSA) were performed to investigate the mechanism underlying the activation effect on the anthrachamycin biosynthetic gene cluster. This work indicated that the *rpoB*-specific missense H437Y mutation had activated anthrachamycin biosynthesis in *S. chattanoogensis* L10. This may be helpful in the investigation of the pleiotropic regulation system in *Streptomyces*.

**Key words:** *Streptomyces*; Cryptic gene cluster; Site-directed mutagenesis; Secondary metabolism  
<https://doi.org/10.1631/jzus.B1900344>

**CLC number:** Q756

### 1 Introduction

Natural products, also regarded as secondary metabolites, are valuable and reliable sources for medical development. They are widely used in veterinary medicine, human therapies, agriculture, and other areas (Bérday, 2005; Chen et al., 2016). It has

been reported that over 50% of antibiotics have been produced by *Actinomycetes* (Demain, 2014). Genome sequencing projects revealed that *Streptomyces* regularly contains more than 20 putative gene clusters for the biosynthesis of peptides, polyketides, bacteriocins, terpenoids, and other natural products (Staunton and Weissman, 2001; Hopwood, 2006; Moore, 2008; Nett et al., 2009). However, many of these gene clusters are silent, hindering the discovery of new natural products (Chen et al., 2016). In *Streptomyces chattanoogensis* L10 (CGMCC 2644), only a small number of these products have been isolated, as directed by three metabolic pathways. However, more than 30 putative secondary metabolic gene clusters remain silent (Guo et al., 2015; Zhou et al., 2015).

<sup>‡</sup> Corresponding author

\* Project supported by the National Natural Science Foundation of China (Nos. 31520103901 and 3173002)

# Electronic supplementary materials: The online version of this article (<https://doi.org/10.1631/jzus.B1900344>) contains supplementary materials, which are available to authorized users

 ORCID: Yong-Quan LI, <https://orcid.org/0000-0001-6013-4068>

© Zhejiang University and Springer-Verlag GmbH Germany, part of Springer Nature 2019

Because of urgent clinical need, many approaches have been established to expand chemical diversities and clinical application of bioactive molecules in *Streptomyces*. Compared to metabolic engineering or classical random approaches for antibiotic production, ribosome engineering represents both a practicable and economical approach to the enhancement of antibiotic production and to the activation of silent gene clusters (Wang et al., 2008). It uses ribosome-targeting drugs to select strains with mutations in RNA polymerase, ribosome proteins, and translation factors (Fu et al., 2014; Ochi, 2017).

A silent gene cluster was activated when a specific *rpoB* mutation was introduced into *S. chattanoogensis* L10. A novel angucycline-like antibiotic with a moderate antioxidant capacity was isolated. Angucyclines are important antibiotics produced by *Streptomyces* sp., and they achieve structural diversity in glycosylation, amino acid incorporation, ring cleavage and epoxidation (Ma et al., 2015; Bao et al., 2018). Angucyclines have been applied as antitumor agents, antioxidants, and in other bioactive fields (Kharel et al., 2012).

The mechanism underlying this distinct activation by the *rpoB* mutation has also been studied using electrophoretic mobility shift assay (EMSA) and quantitative real-time polymerase chain reaction (qRT-PCR) analysis. The results indicated that both the upregulated expression of genes (involved in pleiotropic regulation on antibiotic production) at the transcriptional levels and the AdpA<sub>ch</sub> (AdpA of *S. chattanoogensis* origin) regulatory effect on the *cha* gene cluster might be responsible for the activation of anthracycline biosynthesis.

## 2 Materials and methods

### 2.1 Strains and media

The bacterial strains used in this study are listed in Table S1. *S. chattanoogensis* L10 and its derivatives were grown at 28 °C on yeast extract-malt extract-glucose (YMG) solid medium. Trypticase soy broth was used for extracting genomic DNA (Du et al., 2011). *Escherichia coli* DH5 $\alpha$  and *E. coli* BL21 (DE3) were used as cloning and expression hosts, respectively. *E. coli* cells were cultured in Luria-Bertani

broth (LB) medium with the appropriate concentration of antibiotics for propagating plasmids.

### 2.2 Construction of the plasmids and mutant strains

All plasmids and primers used in this study are listed in Tables S1 and S2, respectively. The site-directed mutagenesis plasmids were constructed following the method of Okamoto-Hosoya et al. (2003), with slight modifications. *rpsL* and *rpoB* were amplified with primer pairs F1/R1 and F2/R2, respectively. The resulting DNA fragments were sequenced and cloned into the *EcoRI/EcoRV* site of pKC1139 (Muth et al., 1989), generating the recombinant plasmids pKC1139-*rpsL* and pKC1139-*rpoB*, respectively. These plasmids were used as templates for the following experiments as illustrated in Fig. S1. After the second round of PCR and digestion with *EcoRI* and *HindIII*, the fragments were ligated into pKC1139. The obtained plasmids were sequenced, harboring the desired mutation in *rpsL* or *rpoB*, to yield the replicating plasmids pKCmu1 to pKCmu10. The pKC1139-based mutational cloning plasmids were introduced into *S. chattanoogensis* L10 by conjugation according to standard procedures (Mao et al., 2015). The mutant strains were selected after double crossover. The coding regions of *rpsL* or *rpoB* in the mutant strains were determined by DNA sequencing analysis, confirming that the wild-type gene was substituted with the mutant allele via homologous recombination.

*chaA* was knocked out by an in-frame deletion in ZJUY1. Two 1-kb DNA fragments flanking the *chaA* coding region were amplified with primer pairs F13/R13 and F14/R14, respectively. The resulting DNA fragments were digested with *HindIII/XbaI* and *XbaI/EcoRV*, respectively, and then sequenced and ligated into pKC1139, generating pKC1139- $\Delta$ *chaA*. The plasmid was then introduced into ZJUY1 via *E. coli* ET12567/pUZ8002 (Mao et al., 2015). The double crossover mutants were screened for apramycin-sensitivity and confirmed by PCR. The *chaA* mutant was named ZJUY11.

*chal* was knocked out using an in-frame deletion in ZJUY1. Two 1-kb DNA fragments flanking the *chal* coding region were amplified with the primer pairs F27/R27 and F28/R28, respectively. The resulting DNA fragments were digested with *XbaI/HindIII* and *XbaI/EcoRI*, respectively, sequenced and ligated

into pKC1139, generating pKC1139- $\Delta$ *chaI*. The plasmid was then introduced into ZJUY1 by conjugation according to standard procedures (Mao et al., 2015). The double crossover mutants were screened for apramycin-sensitivity and confirmed by PCR. The *chaI* mutant was named ZJUY12.

The coding region of *adpA<sub>ch</sub>* was amplified with primer pair F15/R15 and sequentially cloned into the *EcoRI/HindIII* site of pET32a to generate the expression plasmid pET32a-*adpA<sub>ch</sub>*. The promoter region of *chaI* was amplified with the primer pair F17/R17 and cloned into a pClone 007 Blunt Simple Vector (Tsingke, Hangzhou, China) to obtain pClone1 for the promoter-probing assay. All the PCR reactions were conducted with KOD Plus-Neo (Toyobo, Osaka, Japan).

### 2.3 HPLC analysis of anthrachamycin

A 0.5-mL aliquot of the culture was extracted with 0.5 mL of ethyl acetate three times. To compare the metabolic profiles, the crude extracts of different strains were separately filtered and injected into an Agilent 1260 high-performance liquid chromatography (HPLC) system (Agilent, Beijing, China) fitted with an Eclipse Plus XDB-C18 column (5  $\mu$ m,  $\phi$ 4.6 mm $\times$ 150 mm) at a flow rate of 1 mL/min and ultraviolet (UV) detection at 316 nm. We used chromatography with a linear gradient from 5% to 44% (v/v) acetonitrile over 35 min, with a subsequent isocratic stage of 100% acetonitrile for 5 min. The column was further equilibrated with 5% (v/v) acetonitrile for 5 min.

### 2.4 Fermentation and isolation of anthrachamycin

*S. chattanoogensis* L10 and its derivative strains were cultured on YMG solid medium. After incubation for 7 d at 28 °C, spores collected from YMG plates were inoculated into a rotary shaker with 35 mL TNG (15 g/L tryptone, 10 g/L NaCl, 17.5 g/L glucose) medium (Liu et al., 2015) and incubated at 220 r/min and 30 °C for 18 h. The obtained seed culture was added to 35 mL yeast extract-malt extract (YEME) medium to give an optical density at 600 nm ( $OD_{600}$ ) of 0.15. This was fermented at 30 °C in one 250-cm<sup>3</sup> flask for 5 d. The culture was harvested at different time points for RNA preparation or metabolic analysis.

For large-scale fermentation, the obtained seed culture was incubated in two 1000-cm<sup>3</sup> flasks (each with 4 mL of pre-culture) containing liquid TNG

medium (200 mL). The second seed culture was incubated at 220 r/min and 30 °C for 24 h and then transferred into a 15-L stirred tank fermenter with 7.5 L YEME medium. Fermentation was carried out at 250 r/min and 30 °C for 5 d with an air-flow rate of 1 m<sup>3</sup>/(m<sup>3</sup>·min).

The fermentation broth was centrifuged at 3500g for 40 min. The resulting mycelial sediment was washed three times with methanol, and the supernatant was extracted with ethyl acetate three times. Both extracts were mixed and evaporated to dryness under vacuum at 40 °C, which afforded 12.3 g of dark solid. The solid was purified by CombiFlash<sup>®</sup> chromatography with an 8:1 ethyl acetate/methanol mixture as an eluent. The product was purified using a Lumtech semi-preparative HPLC apparatus (column: Agilent XDB-C18, 5  $\mu$ m,  $\phi$ 9.4 mm $\times$ 250 mm; eluent: solvent A 0.1% (v/v) formic acid in water, solvent B 0.1% (v/v) formic acid in acetonitrile; isocratic gradient: 28% (v/v) acetonitrile; flow rate: 3 mL/min) to yield anthrachamycin. After concentration in vacuo to dryness at 20 °C, a yield of 15.0 mg anthrachamycin was obtained.

### 2.5 Structure elucidation

High-resolution electrospray ionization mass spectrometry (HRESI-MS) was recorded using an AB Sciex 5600 QTOF system (AB Sciex, Framingham, MA, USA). Nuclear magnetic resonance (NMR) spectra were gained using a Bruker Advance 600 spectrometer (Bruker Biospin, Milton, Canada). Anthrachamycin was dissolved in dimethyl sulfoxide-*d*<sub>6</sub> (DMSO-*d*<sub>6</sub>) for NMR experiments. The optical rotations were obtained on a PerkinElmer-341 polarimeter (PerkinElmer, Boston, USA). Anthrachamycin: C<sub>31</sub>H<sub>32</sub>O<sub>15</sub>; amorphous red solid; <sup>1</sup>H NMR (600 MHz, DMSO-*d*<sub>6</sub>) and <sup>13</sup>C NMR (600 MHz, DMSO-*d*<sub>6</sub>) (Table S3); infrared spectroscopy (IR; KBr)  $\tilde{\nu}_{\max}$ =3384, 2910, 1624, 1458, 1386, 1078 cm<sup>-1</sup>; UV/Vis (methanol)  $\lambda_{\max}$ =235, 264, 316, 428 nm; (+)-ESI-MS *m/z* 667.25 [M+Na]<sup>+</sup>, (-)-ESI-MS *m/z* 643.05 [M-H]<sup>-</sup>; (+)-HRESI-MS *m/z* 667.1641 [M+Na]<sup>+</sup>, calculated 667.1633.

### 2.6 ABTS assay

The radical scavenging activity of anthrachamycin was evaluated by the 2,2'-azino-bis-(3-ethylbenzthiazoline-6-sulfonic acid) diammonium salt (ABTS) radical cation (ABTS<sup>•+</sup>) assay following the methods of Erel (2004). A total of 200  $\mu$ L of reagent 1

(0.4 mol/L acetate buffer, pH 5.8), 5  $\mu$ L of sample (different concentrations of anthrachamycin and ascorbic acid both dissolved in DMSO), and 20  $\mu$ L of reagent 2 (the ABTS in 30 mmol/L acetate buffer, pH 3.6) were mixed. After 5 min, the decrease in absorbance at 660 nm was monitored. The ABTS<sup>•+</sup> radical scavenging activity of anthrachamycin is expressed as mg vitamin C equivalent (VCE)/g lyophilized powder (LP). All reactions were performed in triplicate.

## 2.7 FRAP assay

The measurement of the ferric reducing capacity of anthrachamycin follows the method of Floegel et al. (2011) and Bao et al. (2016) with modifications. A total of 20  $\mu$ L of anthrachamycin was mixed with 700  $\mu$ L of ferric-reducing antioxidant power (FRAP) solution. The mixture was then incubated at 37 °C for 30 min, and the absorbance was measured at 593 nm. The FRAP values of different concentrations of anthrachamycin were expressed as the known concentrations of mixtures with ferrous ions. All reactions were performed in triplicate.

## 2.8 RNA isolation and qRT-PCR

RNA samples of *S. chattanoogensis* strains were isolated from YEME liquid culture. RNA was prepared following the method of Liu et al. (2015) and Wang et al. (2017). Genomic DNA contamination was diminished by RNase-free DNase I (TaKaRa, Tokyo, Japan). The DNA contamination was confirmed by PCR. RNA was transcribed to complementary DNA (cDNA) with Moloney murine leukemia virus (M-MLV; RNase H<sup>-</sup>, TaKaRa). qRT-PCR was performed using SYBR Premix Ex Taq II (TaKaRa). The primer pairs F18/R18, F19/R19, F20/R20, F21/R21, F22/R22, F23/R23, F24/R24, F25/R25, and F26/R26 were used to detect the transcriptional levels of *relA*, *relC*, *chaA*, *chaGT1*, *chaM*, *chaS*, *chaI*, *adpA*, and *hrdB*, respectively. The transcription of *hrdB* was used as an internal reference. The fold changes of *relA*, *relC*, *chaA*, *chaGT1*, *chaM*, *chaS*, *chaI*, and *adpA* expression were quantified as  $2^{-\Delta\Delta C_T}$  according to the instruction (TaKaRa). All reactions were performed in triplicate.

## 2.9 Expression and purification of AdpA<sub>ch</sub>

*E. coli* BL21 (DE3) carrying pET32a-*adpA<sub>ch</sub>* was cultured in LB medium at 37 °C to OD<sub>600</sub>=0.6

and induced with 0.01 mmol/L isopropyl thiogalactoside (IPTG) for further 18 h at 16 °C. Cells were collected and disrupted by ultrasonication in buffer A (pH 8.0, 50 mmol/L Tris, 500 mmol/L NaCl, 10 mmol/L imidazole). The supernatant was then obtained by centrifugation (13000g for 50 min). Soluble His<sub>6</sub>-TrxA-AdpA<sub>ch</sub> (AdpA<sub>ch</sub>) was purified with nickel-nitrilotriacetic acid (Ni-NTA) His Bind resin (Novagen, Wisconsin, USA) chromatography following the manufacturer's instructions and eluted in buffer B (buffer A plus 250 mmol/L imidazole).

## 2.10 Electrophoretic mobility shift assay

The 5' end with 6-carboxyfluorescein (FAM)-labeled probes were amplified with primer pair F16/R16 from the corresponding plasmids. These probes were gel-purified and eluted in sterile water. About 400 ng of probes were incubated with proteins at 30 °C for 30 min in buffer (100 mmol/L Na<sub>2</sub>HPO<sub>4</sub> (pH 8.0), 20 mmol/L Tris (pH 7.5), 50  $\mu$ g/mL sheared sperm DNA, and 5% (v/v) glycerol). Reactions were performed on 5% (0.05 g/mL) acrylamide gels in a 0.5 $\times$  Tris-borate/ethylenediaminetetraacetic acid (TBE) running buffer and run at 100 V for 1.5 h on ice.

## 3 Results

### 3.1 Introduction of mutations into *rpsL* or *rpoB*

Some specific mutations in *rpsL* or *rpoB* may exhibit positive effects on cryptic gene clusters in *Streptomyces* (Hu et al., 2002; Okamoto-Hosoya et al., 2003; Ochi, 2017). To activate silent gene clusters in *S. chattanoogensis* L10, we constructed mutant strains ZJUY1 to ZJUY10 by introducing specific point mutations into *rpsL* or *rpoB*. Compared to the wild-type strain and other mutants, ZJUY1 accumulated a dark pigment on YMG solid medium (Fig. 1). The HPLC profiles of different strains also indicated that new metabolites were formed in ZJUY1 (Fig. 2). To investigate novel metabolites in ZJUY1 and avoid repetitive research on the compound as in previous studies (Guo et al., 2015), some peaks with novel UV absorptions were prioritized for further investigation.

### 3.2 Elucidation of anthrachamycin

Anthrachamycin was isolated as an amorphous red solid, which displayed a negative specific rotation

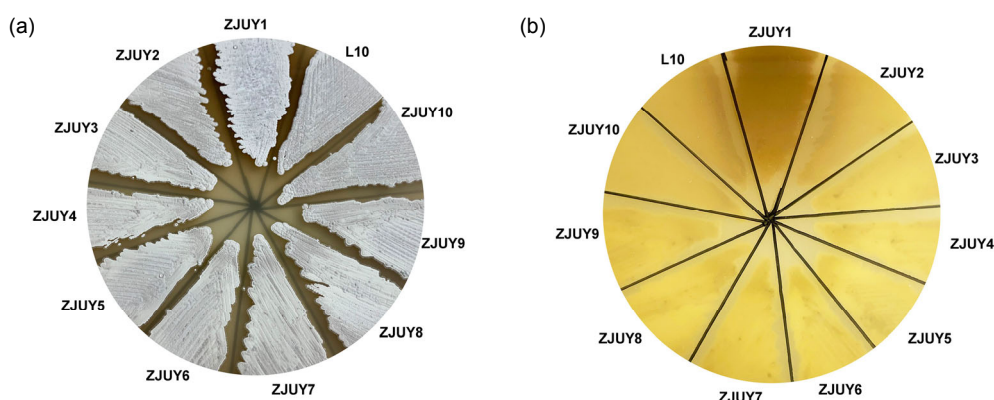


**Fig. 1 Morphological development of L10 and ZJUY1–ZJUY10**

Spores of all strains were patched on the yeast extract-malt extract-glucose (YMG) medium for 7 d. (a) The above side of plate; (b) The reverse side of plate

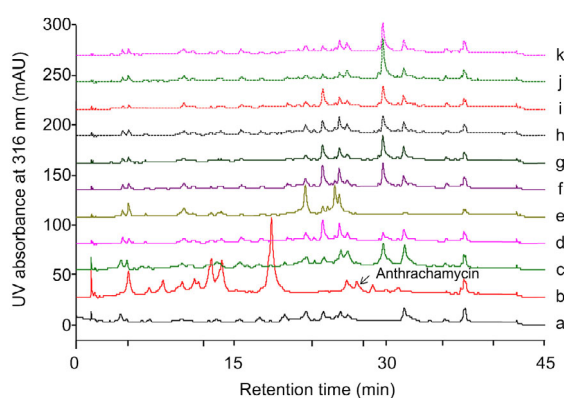


**Fig. 2 HPLC analysis of the crude extracts of L10 and ZJUY1–ZJUY10**

Crude extracts of L10 (a), ZJUY1 (b), ZJUY2 (c), ZJUY3 (d), ZJUY4 (e), ZJUY5 (f), ZJUY6 (g), ZJUY7 (h), ZJUY8 (i), ZJUY9 (j), ZJUY10 (k). The detection wavelength was 316 nm

( $[\alpha]_D^{25} -1.60$ , ( $c$  0.25, DMSO)). HRESI-MS revealed the molecular formula as  $C_{31}H_{32}O_{15}$  ( $m/z$  667.1641  $[M+Na]^+$ , calculated 667.1633) with sixteen unsaturation degrees. The IR spectrum of anthrachamycin showed an absorption band at  $3384\text{ cm}^{-1}$  (hydroxyl group). The one-dimensional (1D) and 2D NMR spectra (Table S3 and Figs. S2–S9) revealed 6  $sp^2$ -hybridized methines, 10  $sp^3$ -hybridized methines, 2  $sp^3$ -hybridized methylenes, 1  $sp^3$ -hybridized methyl, and 12 quaternary carbons. The  $^1\text{H}$  NMR of anthrachamycin revealed two phenolic hydroxyl protons ( $\delta_H=11.56$ ) and six aromatic protons ( $\delta_H=7.80$ , 7.50, 7.46, 7.31, 7.29, 7.01). The heavy metal binding

capacity (HMBC) signals C-2/13-H<sub>3</sub>, C-4/13-H<sub>3</sub>, C-13/2-H, and C-13/4-H revealed a methyl group attached to C-3 (Fig. 3a). Ring A and ring B were connected by the quaternary carbons  $\delta_C=139.7$  (C-4a) and  $\delta_C=115.8$  (C-12b) with HMBC signals C-4a/H-4, C-12b/H-2, and C-12b/H-5. Ring C showed connectivity with ring B through the HMBC signal C-6a/H-5. The typical carbonyl chemical shifts ( $\delta=191.5$  and  $\delta=185.3$ ) indicated the structure of ring C as quinone. The connection between ring C and ring D was highlighted by the HMBC signals C-7a/H-9, C-11a/H-10, and C-12/H-11. Ring D showed a phenolic hydroxyl group and correlated spectroscopy (COSY) signals 9-H/10-H and 10-H/11-H. The HMBC signals in ring D supported the phenolic group at C-8. The gross structure of the aglycone of anthrachamycin was determined by analysis of the NMR data and by comparison with the NMR data of dehydrabelomycin (Lombó et al., 2009) and amycomycin B (Guo et al., 2012). The  $^1\text{H}$  NMR of anthrachamycin revealed two distinct signals for anomeric protons at  $\delta_H=4.92$  and  $\delta_H=4.35$  and the 1H-1H coupling constants  $J(1'-\text{H}, 2'-\text{H})=5.9$  and  $J(1''-\text{H}, 2''-\text{H})=7.8$ , which indicated the presence of two  $\beta$ -sugars. Comparison of our findings with the literature (Francis et al., 1998; El-Toumy et al., 2012) indicated the two sugars as glucopyranoses. The HMBC signals C-1/H-1', C-3'/H-1'' and nuclear overhauser enhancement spectroscopy (NOESY) signal 3'-H/1''-H (Fig. 3b) indicated that a glycosyl moiety was attached to C-1 and that the link is glucose (1 $\rightarrow$ 3).

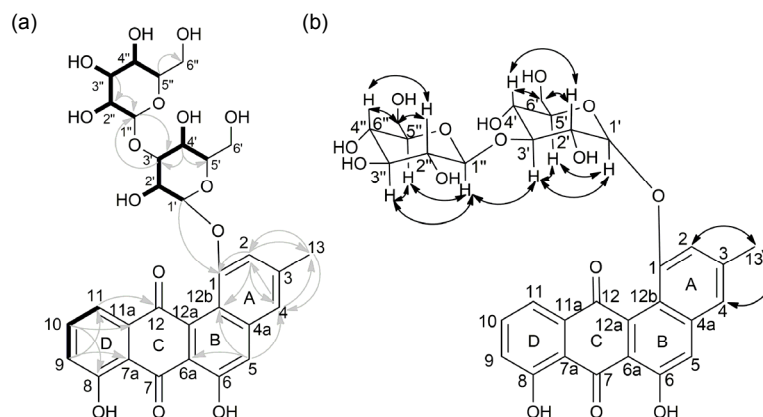


**Fig. 3** 2D NMR analysis of anthrachamycin

(a) Selected HMBC (→) and COSY (bond) correlations of anthrachamycin. (b) Selected NOESY correlations of anthrachamycin. NMR: nuclear magnetic resonance; HMBC: heavy mental binding capacity; COSY: correlated spectroscopy; NOESY: nuclear overhauser enhancement spectroscopy

Based on the above evidence, anthrachamycin was identified as dehydrabelomycin-1-*O*- $\beta$ -glucopyranosyl-(1 $\rightarrow$ 3)- $\beta$ -glucopyranoside. The structure of anthrachamycin resembles those of amycomycin B (dehydrabelomycin-11-*O*- $\alpha$ -rhamnopyranoside) and actinosporin C (dehydrabelomycin-1-*O*- $\alpha$ -rhamnopyranose-8-*O*- $\alpha$ -rhamnopyranoside) (Grkovic et al., 2014), while the glycosylation position and the substituents of sugar moieties of these angucyclines are different. To the best of our knowledge, this work represents the first isolation of anthrachamycin from nature.

### 3.3 Antioxidant activity of anthrachamycin

Anthrachamycin exhibited no inhibitory effect against human HepG2 hepatoma or human MCF-7 breast cancer cell lines (data not shown) and no antimicrobial activity against *Staphylococcus aureus* ATCC 25923, *E. coli* K12, *Bacillus subtilis* ATCC 67736, or *Saccharomyces cerevisiae* BY4741 (data not shown). The antioxidant activity of anthrachamycin was evaluated by ABTS and FRAP assays. In the ABTS assay, the antioxidant activity of anthrachamycin was 67.28 mg VCE/g LP. In the FRAP assay, the antioxidant activity of anthrachamycin was 24.31 mg VCE/g LP. Moreover, anthrachamycin showed a concentration-dependent response in both ABTS (Fig. 4a) and FRAP (Fig. 4b) antioxidant assays. These results indicate that anthrachamycin has a moderate antioxidant capacity, which is similar to the result that the analogue actinosporin C exhibits potent antioxidant activity in the FRAP assay (Grkovic et al., 2014).

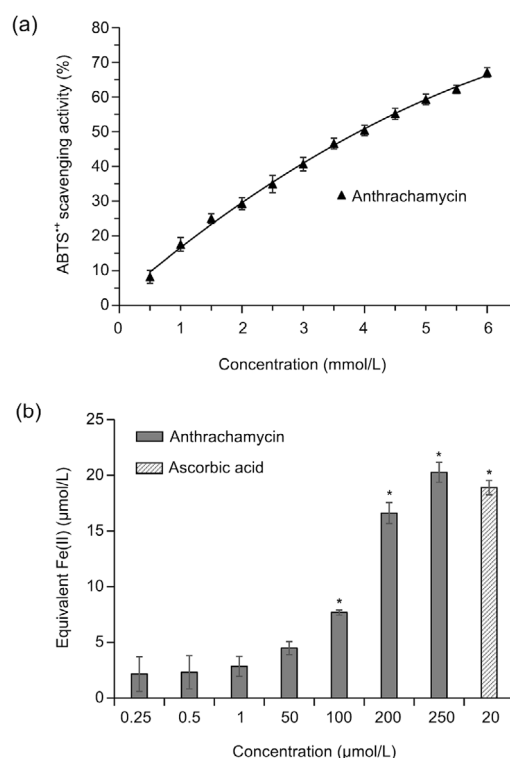


**Fig. 4** Antioxidant activity assay of anthrachamycin

(a) Antioxidant capacity of anthrachamycin was measured using 2,2'-azinobis-(3-ethylbenzthiazoline-6-sulphonate) (ABTS) assay. The results are expressed as arithmetic mean $\pm$ standard deviation ( $n=3$ ). (b) The ferric-reducing antioxidant power (FRAP) of cell-free solutions of anthrachamycin was assessed using photometric quantification (\* $P<0.05$ , significantly different from control (DMSO)). The results are expressed as arithmetic mean $\pm$ standard deviation ( $n=3$ ). Ascorbic acid was used as an antioxidant standard

### 3.4 A cryptic gene cluster activated in a *rpoB* mutant strain

Angucyclines are type II polyketide synthetase (PKS)-engineered natural products (Kharel et al., 2012). Based on the genomic analysis of *S. chattanoogensis* L10, a landomycin analog PKS gene cluster named *cha* (Zhou et al., 2015) was assumed to be responsible for the biosynthesis of anthrachamycin. To validate this gene cluster, we constructed a strain of ZJUY11 ( $\Delta$ *chaA*/RpoB (H437Y)) by deleting the corresponding PKS  $\alpha$ -subunit gene *chaA* in ZJUY1. HPLC analysis indicated the abolishment of anthrachamycin production in ZJUY11 (Fig. 5). The transcriptional levels of selected genes in *cha* gene cluster were examined in ZJUY1 and the wild-type strain by qRT-PCR analysis (*chaM* representing the post-PKS genes; *chaI* as a pathway-specific regulator; *chaA* on behalf of the minimal PKS genes; *chaGT1* standing for the glycosyltransferase genes; *chaS* representing the deoxyhexose genes). At 24 h, the transcript levels of *chaM*, *chaI*, *chaA*, *chaGT1*, and *chaS* from ZJUY1 were about 5.2, 13.8, 86.2, 23.7, and 62.3 times that of the wild-type strain, respectively (Fig. 6). At 36 h, the transcript levels of *chaM*, *chaI*, *chaA*, *chaGT1*, and *chaS* in ZJUY1 were about 3.4, 6.6, 18.8, 20.4, and 32.1 times that of the wild-type strain, respectively. These results indicated that these genes within the *cha* gene cluster were highly expressed at the transcriptional levels in ZJUY1 at 24 and 36 h.

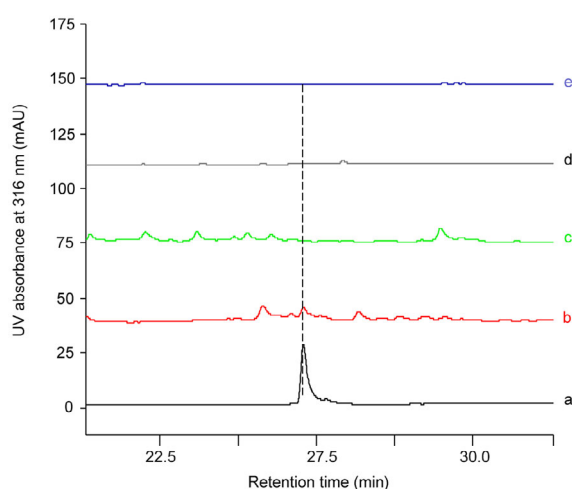


**Fig. 5 HPLC analysis of the crude extracts of ZJUY1, L10, ZJUY11, and ZJUY12**

(a) Authentic samples of anthrachamycin. (b–e) Crude extracts of ZJUY1 (b), L10 (c), ZJUY11 (d), and ZJUY12 (e). The detection wavelength was 316 nm

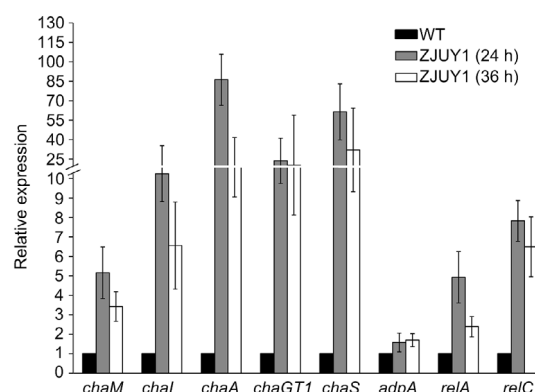


**Fig. 6 Transcriptional analysis of *chaM*, *chaI*, *chaA*, *chaGT1*, *chaS*, *adpA*, *relA*, and *relC* by qRT-PCR**

All RNA samples were isolated from 24 or 36 h in yeast extract-malt extract (YEME) medium. *hrdB* transcription was monitored and used as internal control. Relative expression was shown as expression ratio (arithmetic mean) of *chaM*, *chaI*, *chaA*, *chaGT1*, *chaS*, *adpA*, *relA*, or *relC* to *hrdB* as measured in three independent experiments. All the standard deviations (SDs) are shown as error bars. WT: wild type

In *Streptomyces lividans* and *Streptomyces coelicolor* A3(2), specific *rif* mutations can activate the biosynthesis of actinorhodin, indicating that the *rif* mutation pleiotropically regulates antibiotic biosynthesis (Hu et al., 2002). To investigate the mechanism activating anthrachamycin biosynthesis, we detected the transcript levels of three widely presented genes which may be involved in pleiotropic regulation on secondary metabolism: *relA* (ppGpp (guanosine 5'-diphosphate 3'-diphosphate) synthetase gene), *relC* (encoding ribosomal protein L11), and *adpA* (encoding a pleiotropic regulator AdpA) in ZJUY1 and in the wild-type strain. The transcriptional levels of *relA* and *relC* were both increased more than two times at 24 and 36 h in ZJUY1 (Fig. 6) compared to that of the wild-type strain. Moreover, the transcriptional level of *adpA* was marginally increased during the early stage for secondary metabolism in ZJUY1. Interestingly, the production of landomycin A (a glycosylated angucycline) was enhanced when several heterologous *adpA* genes were overexpressed in *Streptomyces cyanogenus* S136 (Yushchuk et al., 2018). Yushchuk et al. (2018) also believed that the positive effect of *adpA* overexpression on landomycin biosynthesis is mediated by the *lanI*. Given that anthrachamycin is biosynthesized by enzymes encoded

in the *cha* gene cluster and the transcriptional levels of *adpA* and *chal* were increased at 24 and 36 h for secondary metabolism in ZJUY1, we speculate that AdpA<sub>ch</sub> may be also involved in the regulation of *chal*.

### 3.5 *chal*, encoding a putative regulator in *cha* gene cluster

An in silico analysis of the *cha* gene cluster revealed that *chal* encodes a *Streptomyces* antibiotic regulatory protein (SARP) (Rebets et al., 2005, 2008). The deduced amino acid sequence of ChaI resembles other angucycline biosynthesis positive regulators, such as LanI (52% identity to ChaI) in *S. cyanogenus* S136 (Rebets et al., 2003), JadR1 (57% identity to ChaI) in *Streptomyces venezuelae* ISP5230 (Yang et al., 2001), and LndI (56% identity to ChaI) in *Streptomyces globisporus* 1912 (Rebets et al., 2003). As for LanI and JadR1, ChaI can also be classified as a regulator protein of the OmpR-PhoB subfamily (Fu et al., 2014), with  $\alpha$ -helices and  $\beta$ -folds in their C-terminal regions and specific winged helix structures, responsible for DNA binding and productive interaction with RNA polymerase (Makino et al., 1996; Martínez-Hackert and Stock, 1997; Rebets et al., 2003). To investigate the function of ChaI, we deleted the *chal* gene in ZJUY1 to obtain ZJUY12 ( $\Delta$ *chal*/RpoB (H437Y)). HPLC analysis indicated the abolishment of the anthrachamycin product in ZJUY12 (Fig. 5), which suggested that *chal* may play an essential role in the biosynthesis of anthrachamycin.

### 3.6 AdpA<sub>ch</sub> binding to upstream of anthrachamycin biosynthetic gene *chal*

In *S. cyanogenus* S136, the AdpA-mediated boost effect on landomycin A production is dependent on the *lanI* gene (Yushchuk et al., 2018). To test whether AdpA<sub>ch</sub> directly regulates *chal*, EMSA was performed. Based on previous studies on AdpA<sub>ch</sub> in *S. chattanoogensis* L10 (Yu et al., 2014), we screened the nucleotide sequence of the promoter region of *chal* with the consensus sequence 5'-TGGCSNGW WY-3' (where W is A or T, S is G or C, Y is T or C, and N is any nucleotide) using a multiple expectation maximization for motif elicitation (MEME) search. When setting the *P*-value to a threshold of less than 0.0001, one potential AdpA binding site could be suggested as TGGCGTGAAC. EMSA data showed that His<sub>6</sub>-TrxA-AdpA<sub>ch</sub> could bind to the promoter

region of *chal* and form complex bands (Fig. 7a), while no shift bands were observed in the control reaction (Fig. 7b). This confirmed the binding specificity of AdpA<sub>ch</sub> to the *chal* promoter (*chalp*) and suggested that AdpA<sub>ch</sub> regulates the transcription of *chal* by specifically binding to the promoter region of *chal*.

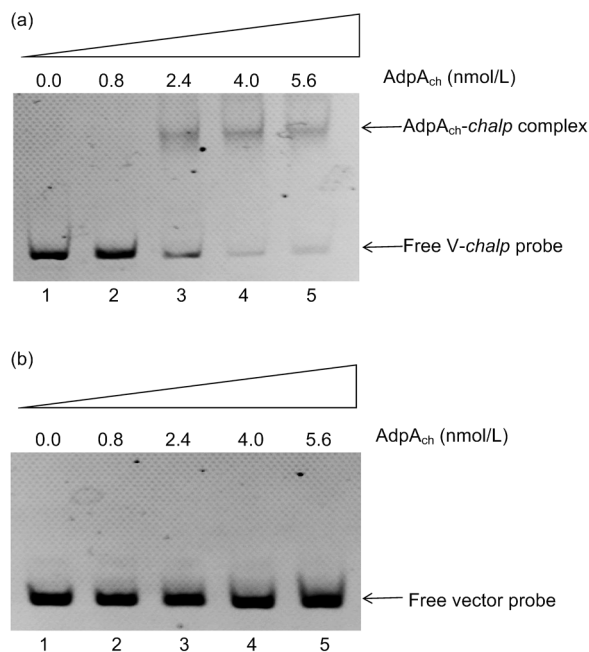


**Fig. 7 AdpA<sub>ch</sub> binding to the *chal* promoter (*chalp*)**

The 5-FAM-labeled *chalp* (V-*chalp*) was used as a probe and the 5-FAM-labeled void vector was a negative control. (a) Lanes 1 to 5, about 4 pmol/L (400 ng) 5-FAM-labeled *chalp* (V-*chalp*) probes from pClone1 with 0, 0.8, 2.4, 4.0, or 5.6 nmol/L of purified His<sub>6</sub>-Trx-AdpA<sub>ch</sub>, respectively. (b) Lanes 1 to 5, about 4 pmol/L (400 ng) 5-FAM-labeled void vector from pClone007 Blunt Simple Vector with 0, 0.8, 2.4, 4.0, or 5.6 nmol/L of purified His<sub>6</sub>-Trx-AdpA<sub>ch</sub>, respectively. FAM: 6-carboxyfluorescein

## 4 Discussion

Ribosome engineering mainly introduces mutations conferring drug resistance and selects various mutant forms based on colony size, morphology, or pigment formation (Ochi, 2017). Differing from the spontaneous generation of drug-resistant mutations, we used site-directed mutagenesis to directly construct target mutant strains and avoid the isolation of multiple colonies. However, the efficiency of this

approach is unpredictable as mutant sites may exhibit different effects on bacterial fitness and the activation of various silent gene clusters (Craney et al., 2013; Tanaka et al., 2013). It has now become feasible to integrate ribosome engineering with other genome mining strategies to improve activation efficiency and activate biosynthetic gene clusters of interest.

The mechanism activating silent genes by *rpoB* mutations in *Streptomyces* is not entirely clear but involves the upregulation expression of cryptic genes at the transcriptional levels (Gomez-Escribano and Bibb, 2011; Ochi, 2017).

AdpA, a transcriptional factor of the AraC/XylS-type regulatory protein family, is widely present in *Streptomyces* genomes and frequently influences the transcription of antibiotic biosynthesis genes both directly and indirectly (Yu et al., 2014; Yushchuk et al., 2018). It has been reported that AdpA positively regulated secondary metabolites biosynthesis by controlling cluster-situated regulators in *Streptomyces griseus* (Ohnishi et al., 1999), *Streptomyces roseosporus* (Mao et al., 2015), *Streptomyces avermitilis* (Komatsu et al., 2010), *Streptomyces clavuligerus* (López-García et al., 2010), and *S. chattanoogensis* (Du et al., 2011). In *S. griseus*, the transcriptional level of *adpA* was found to be impaired in the early and late growth phases when the Q424K mutation was introduced into RpoB. Conversely, the *rsmG* mutation (conferring a low-level resistance to streptomycin) enhanced the expression of *adpA* (Tanaka et al., 2013). Similarly, the transcript level of *adpA* was marginally increased in ZJUY1. EMSA results suggest that AdpA<sub>ch</sub> regulates the transcription of *chaI* by specifically binding to the promoter region of *chaI*. This is consistent with the case that AdpA is involved in landomycin A biosynthetic regulatory network (Yushchuk et al., 2018). Taken together with the results mentioned above, it is possible that the transcriptional level changes in *adpA* and AdpA<sub>ch</sub>'s regulatory effect on *chaI* may influence *cha* cluster expression in ZJUY1.

RelA and RelC are necessary for the biosynthesis of ppGpp, which may participate significantly in the activation of cryptic gene clusters (Hesketh et al., 2001; Inaoka et al., 2004; Ochi, 2017). In *S. coelicolor* A(3)2 and *S. lividans*, alteration at His-437 to Tyr or Arg in RpoB circumvented the detrimental effects of antibiotic production resulting from the lack

of ppGpp due to *relA* or *relC* mutations (Inaoka et al., 2004). In ZJUY1, the transcriptional levels of *relA* and *relC* were also remarkably enhanced. Further work is required to determine the molecular basis for the transcriptional level changes of *relA* and *relC* in RpoB mutant strains.

The results presented in this study revealed that the activation effect on anthrachamycin biosynthesis by the *rpoB* mutation is attributed, at least in part, to the transcriptional changes of the genes corresponding to stringent response and pleiotropic regulation (Fig. S10). Transcriptome and proteome analysis will be performed to further investigate the changes in gene expression and protein biosynthesis in ZJUY1. It is possible that some novel secondary metabolites were activated with low yields in ZJUY2–ZJUY10 and further studies are required to enhance the activation efficiency and detect the novel metabolites of silent gene clusters.

## 5 Conclusions

In this study, a silent gene cluster was activated when we used site-directed mutagenesis to generate an RpoB mutation in *S. chattanoogensis* L10. After further investigation into the metabolites of L10/RpoB (H437Y), a novel angucycline-like antibiotic named anthrachamycin was isolated. qRT-PCR and EMSA were performed to further investigate the mechanism underlying the activation effect on the anthrachamycin biosynthetic gene cluster. The work presented here will be helpful towards further investigation of the pleiotropic regulation system in *Streptomyces*.

## Contributors

Zi-yue LI, Qing-ting BU, Jue WANG, and Yu LIU performed the experiments. Zi-yue LI and Qing-ting BU wrote the manuscript. Xin-ai CHEN, Xu-ming MAO, and Yong-Quan LI revised the manuscript. All authors read and approved the final manuscript. Therefore, all authors had full access to all the data in the study and take responsibility for the integrity and security of the data.

## Compliance with ethics guidelines

Zi-yue LI, Qing-ting BU, Jue WANG, Yu LIU, Xin-ai CHEN, Xu-ming MAO, and Yong-Quan LI declare that they have no conflict of interest.

This article does not contain any studies with human or animal subjects performed by any of the authors.

## References

- Bao J, He F, Li YM, et al., 2018. Cytotoxic antibiotic angucyclines and actinomycins from the *Streptomyces* sp. XZHG99T. *J Antibiot (Tokyo)*, 71(12):1018-1024. <https://doi.org/10.1038/s41429-018-0096-1>
- Bao T, Wang Y, Li YT, et al., 2016. Antioxidant and antidiabetic properties of tartary buckwheat rice flavonoids after in vitro digestion. *J Zhejiang Univ-Sci B (Biomed & Biotechnol)*, 17(12):941-951. <https://doi.org/10.1631/jzus.B1600243>
- Bérdy J, 2005. Bioactive microbial metabolites. *J Antibiot (Tokyo)*, 58(1):1-26. <https://doi.org/10.1038/ja.2005.1>
- Chen JW, Wu QH, Hawas UW, et al., 2016. Genetic regulation and manipulation for natural product discovery. *Appl Microbiol Biotechnol*, 100(7):2953-2965. <https://doi.org/10.1007/s00253-016-7357-3>
- Craney A, Ahmed S, Nodwell J, 2013. Towards a new science of secondary metabolism. *J Antibiot (Tokyo)*, 66(7):387-400. <https://doi.org/10.1038/ja.2013.25>
- Demain AL, 2014. Importance of microbial natural products and the need to revitalize their discovery. *J Ind Microbiol Biotechnol*, 41(12):185-201. <https://doi.org/10.1007/s10295-013-1325-z>
- Du YL, Shen XL, Yu P, et al., 2011. Gamma-butyrolactone regulatory system of *Streptomyces chattanoogensis* links nutrient utilization, metabolism, and development. *Appl Environ Microbiol*, 77(23):8415-8426. <https://doi.org/10.1128/AEM.05898-11>
- El-Toumy SA, El Souda SS, Mohamed TK, et al., 2012. Anthraquinone glycosides from *Cassia roxburghii* and evaluation of its free radical scavenging activity. *Carbohydr Res*, 360:47-51. <https://doi.org/10.1016/j.carres.2012.07.020>
- Erel O, 2004. A novel automated direct measurement method for total antioxidant capacity using a new generation, more stable ABTS radical cation. *Clin Biochem*, 37(4):277-285. <https://doi.org/10.1016/j.clinbiochem.2003.11.015>
- Floegel A, Kim DO, Chung SJ, et al., 2011. Comparison of ABTS/DPPH assays to measure antioxidant capacity in popular antioxidant-rich US foods. *J Food Compos Anal*, 24(7):1043-1048. <https://doi.org/10.1016/j.jfca.2011.01.008>
- Francis GW, Aksnes DW, Holt Ø, 1998. Assignment of the <sup>1</sup>H and <sup>13</sup>C NMR spectra of anthraquinone glycosides from *Rhamnus frangula*. *Magn Reson Chem*, 36(10):769-772. [https://doi.org/10.1002/\(SICI\)1097-458X\(199810\)36:10<769::AID-OMR361>3.0.CO;2-E](https://doi.org/10.1002/(SICI)1097-458X(199810)36:10<769::AID-OMR361>3.0.CO;2-E)
- Fu P, Jamison M, La S, et al., 2014. Inducamides A-C, chlorinated alkaloids from an RNA polymerase mutant strain of *Streptomyces* sp. *Org Lett*, 16(21):5656-5659. <https://doi.org/10.1021/ol502731p>
- Gomez-Escribano JP, Bibb MJ, 2011. Engineering *Streptomyces coelicolor* for heterologous expression of secondary metabolite gene clusters. *Microb Biotechnol*, 4(2):207-215. <https://doi.org/10.1111/j.1751-7915.2010.00219.x>
- Grkovic T, Abdelmohsen UR, Othman EM, et al., 2014. Two new antioxidant actinosporin analogues from the calcium alginate beads culture of sponge-associated *Actinokineospora* sp. strain EG49. *Bioorg Med Chem Lett*, 24(21):5089-5092. <https://doi.org/10.1016/j.bmcl.2014.08.068>
- Guo YY, Li H, Zhou ZX, et al., 2015. Identification and biosynthetic characterization of natural aromatic azoxy products from *Streptomyces chattanoogensis* L10. *Org Lett*, 17(24):6114-6117. <https://doi.org/10.1021/acs.orglett.5b03137>
- Guo ZK, Liu SB, Jiao RH, et al., 2012. Angucyclines from an insect-derived actinobacterium *Amycolatopsis* sp. HCa1 and their cytotoxic activity. *Bioorg Med Chem Lett*, 22(24):7490-7493. <https://doi.org/10.1016/j.bmcl.2012.10.048>
- Hesketh A, Sun J, Bibb M, 2001. Induction of ppGpp synthesis in *Streptomyces coelicolor* A3(2) grown under conditions of nutritional sufficiency elicits actII-ORF4 transcription and actinorhodin biosynthesis. *Mol Microbiol*, 39(1):136-144. <https://doi.org/10.1046/j.1365-2958.2001.02221.x>
- Hopwood DA, 2006. Soil to genomics: the *Streptomyces* chromosome. *Annu Rev Genet*, 40:1-23. <https://doi.org/10.1146/annurev.genet.40.110405.090639>
- Hu HF, Zhang Q, Ochi K, 2002. Activation of antibiotic biosynthesis by specified mutations in the *rpoB* gene (encoding the RNA polymerase β subunit) of *Streptomyces lividans*. *J Bacteriol*, 184(14):3984-3991. <https://doi.org/10.1128/JB.184.14.3984-3991.2002>
- Inaoka T, Takahashi K, Yada H, et al., 2004. RNA polymerase mutation activates the production of a dormant antibiotic 3,3'-neotrehalosadiamine via an autoinduction mechanism in *Bacillus subtilis*. *J Biol Chem*, 279(5):3885-3892. <https://doi.org/10.1074/jbc.M309925200>
- Kharel MK, Pahari P, Shepherd MD, et al., 2012. Angucyclines: biosynthesis, mode-of-action, new natural products, and synthesis. *Nat Prod Rep*, 29(2):264-325. <https://doi.org/10.1039/c1np00068c>
- Komatsu M, Uchiyama T, Omura S, et al., 2010. Genomeminimized *Streptomyces* host for the heterologous expression of secondary metabolism. *Proc Natl Acad Sci USA*, 107(6):2646-2651. <https://doi.org/10.1073/pnas.0914833107>
- Liu SP, Yu P, Yuan PH, et al., 2015. Sigma factor WhiG<sub>ch</sub> positively regulates natamycin production in *Streptomyces chattanoogensis* L10. *Appl Microbiol Biotechnol*, 99(6):2715-2726. <https://doi.org/10.1007/s00253-014-6307-1>
- Lombó F, Abdelfattah MS, Braña AF, et al., 2009. Elucidation of oxygenation steps during oviedomycin biosynthesis and generation of derivatives with increased antitumor

- activity. *ChemBioChem*, 10(2):296-303.  
<https://doi.org/10.1002/cbic.200800425>
- López-García MT, Santamarta I, Liras P, 2010. Morphological differentiation and clavulanic acid formation are affected in a *Streptomyces clavuligerus adpA*-deleted mutant. *Microbiology*, 156(8):2354-2365.  
<https://doi.org/10.1099/mic.0.035956-0>
- Ma M, Rateb ME, Teng QH, et al., 2015. Angucyclines and angucyclinones from *Streptomyces* sp. CB01913 featuring C-ring cleavage and expansion. *J Nat Prod*, 78(10):2471-2480.  
<https://doi.org/10.1021/acs.jnatprod.5b00601>
- Makino K, Amemura M, Kawamoto T, et al., 1996. DNA binding of PhoB and its interaction with RNA polymerase. *J Mol Biol*, 259(1):15-26.  
<https://doi.org/10.1006/jmbi.1996.0298>
- Mao XM, Luo S, Zhou RC, et al., 2015. Transcriptional regulation of the daptomycin gene cluster in *Streptomyces roseosporus* by an autoregulator, AtrA. *J Biol Chem*, 290(12):7992-8001.  
<https://doi.org/10.1074/jbc.M114.608273>
- Martínez-Hackert E, Stock AM, 1997. The DNA-binding domain of OmpR: crystal structures of a winged helix transcription factor. *Structure*, 5(1):109-124.  
[https://doi.org/10.1016/S0969-2126\(97\)00170-6](https://doi.org/10.1016/S0969-2126(97)00170-6)
- Moore BS, 2008. Extending the biosynthetic repertoire in ribosomal peptide assembly. *Angew Chem Int Ed Engl*, 47(49):9386-9388.  
<https://doi.org/10.1002/anie.200803868>
- Muth G, Nußbaumer B, Wohlleben W, et al., 1989. A vector system with temperature-sensitive replication for gene disruption and mutational cloning in streptomycetes. *Mol Gen Genet*, 219(3):341-348.  
<https://doi.org/10.1007/bf00259605>
- Nett M, Ikeda H, Moore BS, 2009. Genomic basis for natural product biosynthetic diversity in the actinomycetes. *Nat Prod Rep*, 26(11):1362-1384.  
<https://doi.org/10.1039/b817069j>
- Ochi K, 2017. Insights into microbial cryptic gene activation and strain improvement: principle, application and technical aspects. *J Antibiot (Tokyo)*, 70:25-40.  
<https://doi.org/10.1038/ja.2016.82>
- Ohnishi Y, Kameyama S, Onaka H, et al., 1999. The A-factor regulatory cascade leading to streptomycin biosynthesis in *Streptomyces griseus*: identification of a target gene of the A-factor receptor. *Mol Microbiol*, 34(1):102-111.  
<https://doi.org/10.1046/j.1365-2958.1999.01579.x>
- Okamoto-Hosoya Y, Okamoto S, Ochi K, 2003. Development of antibiotic-overproducing strains by site-directed mutagenesis of the *rpsL* gene in *Streptomyces lividans*. *Appl Environ Microbiol*, 69(7):4256-4259.  
<https://doi.org/10.1128/aem.69.7.4256-4259.2003>
- Rebets Y, Ostash B, Luzhetskyy A, et al., 2003. Production of landomycins in *Streptomyces globisporus* 1912 and *S. cyanogenus* S136 is regulated by genes encoding putative transcriptional activators. *FEMS Microbiol Lett*, 222(1):149-153.  
[https://doi.org/10.1016/S0378-1097\(03\)00258-1](https://doi.org/10.1016/S0378-1097(03)00258-1)
- Rebets Y, Ostash B, Luzhetskyy A, et al., 2005. DNA-binding activity of LndI protein and temporal expression of the gene that upregulates landomycin E production in *Streptomyces globisporus* 1912. *Microbiology*, 151(1):281-290.  
<https://doi.org/10.1099/mic.0.27244-0>
- Rebets Y, Dutko L, Ostash B, et al., 2008. Function of *lanI* in regulation of landomycin A biosynthesis in *Streptomyces cyanogenus* S136 and cross-complementation studies with *Streptomyces* antibiotic regulatory proteins encoding genes. *Arch Microbiol*, 189(2):111-120.  
<https://doi.org/10.1007/s00203-007-0299-5>
- Staunton J, Weissman KJ, 2001. Polyketide biosynthesis: a millennium review. *Nat Prod Rep*, 18(4):380-416.  
<https://doi.org/10.1039/a909079g>
- Tanaka Y, Kasahara K, Hirose Y, et al., 2013. Activation and products of the cryptic secondary metabolite biosynthetic gene clusters by rifampin resistance (*rpoB*) mutations in actinomycetes. *J Bacteriol*, 195(13):2959-2970.  
<https://doi.org/10.1128/JB.00147-13>
- Wang GJ, Hosaka T, Ochi K, 2008. Dramatic activation of antibiotic production in *Streptomyces coelicolor* by cumulative drug resistance mutations. *Appl Environ Microbiol*, 74(9):2834-2840.  
<https://doi.org/10.1128/AEM.02800-07>
- Wang TJ, Shan YM, Li H, et al., 2017. Multiple transporters are involved in natamycin efflux in *Streptomyces chattanoogensis* L10. *Mol Microbiol*, 103(4):713-728.  
<https://doi.org/10.1111/mmi.13583>
- Yang KQ, Han L, He JY, et al., 2001. A repressor-response regulator gene pair controlling jadomycin B production in *Streptomyces venezuelae* ISP5230. *Gene*, 279(2):165-173.  
[https://doi.org/10.1016/S0378-1119\(01\)00723-5](https://doi.org/10.1016/S0378-1119(01)00723-5)
- Yu P, Liu SP, Bu QT, et al., 2014. WblA<sub>ch</sub>, a pivotal activator of natamycin biosynthesis and morphological differentiation in *Streptomyces chattanoogensis* L10, is positively regulated by AdpA<sub>ch</sub>. *Appl Environ Microbiol*, 80(22):6879-6887.  
<https://doi.org/10.1128/AEM.01849-14>
- Yushchuk O, Ostash I, Vlasuk I, et al., 2018. Heterologous AdpA transcription factors enhance landomycin production in *Streptomyces cyanogenus* S136 under a broad range of growth conditions. *Appl Microbiol Biotechnol*, 102(19):8419-8428.  
<https://doi.org/10.1007/s00253-018-9249-1>
- Zhou ZX, Xu QQ, Bu QT, et al., 2015. Genome mining-directed activation of a silent angucycline biosynthetic gene cluster in *Streptomyces chattanoogensis*. *ChemBioChem*, 16(3):496-502.  
<https://doi.org/10.1002/cbic.201402577>

## List of electronic supplementary materials

Table S1 Strains and plasmids used in this study

Table S2 Oligonucleotide primers used in this study

Table S3  $^1\text{H}$  and  $^{13}\text{C}$  NMR data of anthrachamycin in  $\text{DMSO-}d_6$  (600 MHz)

Fig. S1 Schematic representation of overlapping PCR strategy for introducing mutations into *rpsL* or *rpoB*

Fig. S2 UV absorption of anthrachamycin

Fig. S3  $^1\text{H}$  NMR spectrum of anthrachamycin

Fig. S4  $^{13}\text{C}$  NMR spectrum of anthrachamycin

Fig. S5 Distortionless enhancement by polarization transfer (DEPT135) spectrum of anthrachamycin

Fig. S6 Correlated spectroscopy (COSY) spectrum of anthrachamycin

Fig. S7 Nuclear overhauser enhancement spectroscopy (NOESY) spectrum of anthrachamycin

Fig. S8 Heteronuclear single quantum coherence (HSQC) spectrum of anthrachamycin

Fig. S9 Heavy metal binding capacity (HMBC) spectrum of anthrachamycin

Fig. S10 Speculated mechanism for activating anthrachamycin biosynthesis

## 中文概要

题目: 恰塔努加链霉菌 L10 中 *rpoB* 基因突变激活蒽塔恰霉素生物合成基因簇的研究

目的: 运用核糖体技术激活恰塔努加链霉菌 *Streptomyces chattanoogensis* L10 中的隐性基因簇, 进一步研究突变菌株的次级代谢产物并初步探索其对应的生物合成基因簇激活机制。

创新点: 首次分离得到了蒽塔恰霉素, 并初步探索了 RpoB 突变株中蒽塔恰霉素生物合成基因簇的激活机制。

方法: 采用核糖体工程技术, 对 *S. chattanoogensis* L10 的 RpsL 和 RpoB 的高度保守区域定点突变, 使用高效液相色谱法 (HPLC) 检测突变株的代谢产物。运用一维和二维核磁共振 (1D NMR、2D NMR) 解析 L10/RpoB (H437Y) 的次级代谢产物蒽塔恰霉素的化学结构, 通过铁离子还原法 (FRAP) 和 ABTS 自由基清除等实验研究其抗氧化活性。采用实时荧光定量聚合酶链式反应 (qRT-PCR) 和凝胶电泳迁移率分析 (EMSA) 探索蒽塔恰霉素生物合成基因簇的激活机制。

结论: L10/RpoB (H437Y) 中蒽塔恰霉素的生物合成基因簇被激活。qRT-PCR 和 EMSA 结果表明: RNA 聚合酶  $\beta$  亚基结构改变, 可能影响全局性调控基因的转录水平, 并激活蒽塔恰霉素生物合成基因簇。

关键词: 链霉菌; 隐性基因簇; 定点突变; 次级代谢产物